

Research Article

A V2P Collision Risk Warning Method based on LSTM in IOV

Ruoyu Pan ¹, Lihua Jie ¹, Xinyue Zhang ¹, Shengli Pang ¹, Honggang Wang ¹,
and Zhaoying Wei ²

¹Institute of Communication Engineering, Xi'an University of Posts and Telecommunications, Xi'an, China

²Institute of College of Science, Xi'an Shiyou University, Xi'an, China

Correspondence should be addressed to Honggang Wang; wanghonggang@xupt.edu.cn

Received 16 May 2022; Revised 13 June 2022; Accepted 25 June 2022; Published 31 July 2022

Academic Editor: Chen Chen

Copyright © 2022 Ruoyu Pan et al. This is an open access article distributed under the Creative Commons Attribution License, which permits unrestricted use, distribution, and reproduction in any medium, provided the original work is properly cited.

With the evolution of communication networks, the Internet of Vehicles (IOV) continues to accelerate the safe and rapid development of autonomous vehicles. Vehicle-to-Pedestrian (V2P) communication is a key technology in autonomous vehicles and a potential solution to realize collaborative intelligence between vehicles and pedestrians. However, the existing V2P communication early warning system does not consider the uncertainty of pedestrian trajectory, and the determination of the collision area is limited to a single point, resulting in an inaccurate system judgment and limited improvement of traffic efficiency. This paper designs a new autonomous-oriented V2P communication network architecture and completes a V2P communication early warning system based on Long Range (LoRa). A V2P anticollision model is established, and a new V2P collision risk early warning method is proposed. In this method, danger index is introduced into the early warning of collision between pedestrian and vehicle. The long short-term memory (LSTM) artificial neural network is used to predict the pedestrian's trajectory, so as to deduce the pedestrian-vehicle collision risk area when the pedestrian trajectory is uncertain. Meanwhile, the confidence probability is used to judge whether the pedestrian and vehicle are warned. The simulation shows that the V2P collision risk warning method proposed in this paper has good performance, which can accurately warn the pedestrian and vehicle under different vehicle speeds and Global Positioning System (GPS) positioning errors. At the same time, it reflects the characteristics of intelligence brought by using LSTM methods. Using the V2P communication early warning system based on LoRa to verify the experimental results show that when the GPS positioning accuracy is submeter level, the prediction accuracy is greater than 98%. The results of the proposed method show good performance and high detection rate.

1. Introduction

Automated system intelligent control in the automatic driving field is widely used. In recent years, autonomous driving technology has made considerable progress. Academia and industry are actively promoting it around the world, injecting new vitality into the research of autonomous vehicles technology [1, 2]. Self-driving automobiles rely on the collaboration of artificial intelligence, wireless communication, visual computing, radar, surveillance equipment, and global positioning systems, which can automatically and safely drive without manual intervention [3]. Relying on advanced vehicle intelligent control technology, self-driving automobiles not only liberate manpower but also reduce the human error of

drivers and even reduce the incidence of traffic accidents to zero. In addition, self-driving automobiles can encourage people to carpool, greatly reduce the use of cars, increase the capacity of major roads, improve road capacity, and reduce air pollution caused by car exhaust. Therefore, the emergence of self-driving automobiles provides an ideal solution to problems such as traffic accidents, traffic congestion, energy consumption, and environmental pollution.

Vehicles and pedestrians are the main participants in traffic, so V2P is one of the core issues of autonomous driving [4–6]. It can even predict changes in traffic conditions. By exchanging the key information of vehicle and pedestrian directly, the efficiency of road traffic can be effectively improved and the intelligent road environment of

vehicle-road coordination can be realized. It is a key factor for the automobile intelligence.

Automobile intelligence requires vehicles to have the ability to communicate with road users. Automobile intelligence requires accurate acquisition and analysis of the following information to predict the future behavior of road users and generate corresponding responses, including user behavior information such as route, location, speed, and direction. This interaction is crucial between vehicles and pedestrians. The movement of vehicles, such as cars, trucks and buses, is governed by clear rules and environmental conditions. However, as the main participants of road traffic, pedestrians are not considered because of their complex, dynamic, and random behavior [4]. This paper considers the uncertain trajectory factors of the pedestrian and designs a V2P early warning system to effectively improve the accuracy of the warning system.

Pedestrians, cyclists, and motorized two-wheeler operators are called Vulnerable Road Users (VRUs) [7]. The protection of VRUs is a common topic in V2P [8]. Advanced Driver Assistance System (ADAS) uses sensor technology [9–11], the far-infrared method [12], computer vision [13], and a combination of methods [14] to detect pedestrian location information.

Compared with ADAS, the Internet of Vehicles (IOV) can detect the relative motion state of vehicles and pedestrians and perceive potentially dangerous situations more accurately in the case of None Light of Sight (NLOS), to achieve cooperative safety to ensure safer and more efficient transportation. Wireless communication technology is the cornerstone of the development of the IOV, which has been extensively studied by researchers. Different wireless communication technologies have different advantages and disadvantages. As shown in Table 1, LTE towers can cover 16 KM, but their energy consumption is very large and the Doppler effect caused by high carrier frequency is difficult to eliminate [11, 15]. Millimeter-wave (MmWAVE) has abundant bandwidth and short wavelength. At the same time, MmWAVE is an emerging technology that faces many challenges. For example, it is easy to be blocked by obstacles due to the short wavelength, so relayed forwarding is required, but the core problem of rapid selection of the optimal relay has not been solved [16, 17]. Wi-Fi has a high data transmission rate, which usually has a communication range of 100–150 meters. Driving at a speed of 50 km/h can meet the requirements. However, in the suburban areas, with the typical speed of 100 km/h, the requirements cannot be met because drivers have less reaction time to take action. Moreover, Wi-Fi wireless communication transmission cannot achieve low-latency bidirectional communication [18].

While LoRa strikes a balance between transmission range and data transfer rate. A LoRa base station can cover 15 km with data rates ranging from 300 bps to 37.5 kbps, depending on the spreading factor (SF) and channel bandwidth [19]. In addition, the LoRa base station can accommodate 1 million terminals, and simultaneously receive multiple transmissions using different spreading factors. When using a spreading factor of 12, the transmit

power is 14 dB, and the transmission to the base station with a distance of 420 m is 96.7% [20]. Simultaneous reception of multiple spreading factors (between 7 and 12) creates a third possibility beyond time and frequency. In addition, the VRUs protection system of V2P communication requires low-power, low-cost, and small wireless communication equipment to ensure low-latency and high-reliability transmission of data under high bandwidth within the transmission range. Therefore, wearable devices with these characteristics of LoRa wireless communication technology can meet the requirements of VRUs protection system for V2P communication.

Regarding the establishment of anticollision models, many warning systems have been proposed in the existing literature. In [21], a V2X coordination system based on cellular and 802.11 p radio: SafeNav android application is proposed, the interface has set a predetermined collision area, if multiple traffic participants enter the collision area, visual and audible alerts are generated, and the color of the traffic participant changes to red and beep sound is emitted. In [5], a mobile application that supports pedestrians and vehicles was proposed by Hussein et al., the screen is active when the user interacts with the mobile phone to detect the position coordinates of the mobile phone. The system calculates the collision point and determines whether there is a collision. Increase the VRU's visual situational awareness of the location near the automatically and manually controlled vehicles in the form of user-friendly operation. All the above studies require manual intervention and are not highly automated, which may bring certain security risks [22, 23]. Liu et al. developed a warning system POFs, which uses IEEE 802.11 p and Wi-Fi as communication channels to warn pedestrians by predicting collisions and issuing alerts [24]. Ho et al. designed a WIFI-based anticollision system, which encapsulates longitude, latitude, direction, and speed in a service set identifier (SSID) for transmission, and judges whether there is a collision risk by parsing the SSID of vehicles and pedestrians [25]. The warning system based on dedicated short-range communication (DSRC) and Wi-Fi has relatively high accuracy, but the applicable distance is limited. Xiog et al. proposed a graded warning system, which divides the warning into two types: danger warning and emergency braking according to the position coordinates of the pedestrian crossing road [26]. Bastani Zadeh proposed a three-level collision warning system, in which the first stage is used to activate the system to deal with various dangerous situations, the second stage is to extract important features to evaluate the collision risk by using fuzzy reasoning engine, and the third stage is to divide the warning alarms into low, medium, and high risk [27]. The prediction of the future trajectory of pedestrians is necessary to improve the accuracy of the anticollision system because pedestrians, as major participants in road traffic, may change direction suddenly according to external factors such as objects and vehicles [28]. Ideally, a pedestrian's walking destination determines its trajectory; however, in the real world, its destination is not always known. Therefore, it is necessary to learn the behavior characteristics of pedestrians based on the past time trajectory sequence. However, the above methods do not

TABLE 1: Technical parameters of wireless communication.

	Maximum transmission distance	Spectrum	Energy consumption
LTE	16 km	1.25~20 MHz	High
MmWAVE	3.8 km	6~100 GHz	High
WiFi	150 m	2.4 GHz	Low
Zigbee	100 m	2.4 GHz	Low
Bluetooth	50 m	2.4 GHz	Low
LoRa	15 km	433/868/915 MHz	Low

consider the uncertainty of pedestrian trajectory, and the methods for judging collision are limited to whether there is a collision point, which should be an area, rather than a single point. In order to solve the uncertainty problem, introducing the neural network is a suitable choice [29–31]. For the description of the collision area, previous studies mostly used the maximum likelihood solution or the difference between the major and minor axes of the ellipse are used to describe the uncertainty in the position [32, 33].

This paper proposes the early warning system, which adopts LoRa for data transmission and GPS for data acquisition. The main contributions are in two aspects: 1. In the V2P communication problem, the model not only considers whether there is a collision risk from the perspective of strict physical calculation but also introduces a risk index to measure the degree of risk to reduce the judgment error. 2. The algorithm takes the uncertainty of the pedestrian trajectory into the model. In this process, the future uncertainty trajectory of the pedestrian is represented as a collision area given by a confidence ellipse, and the corresponding confidence probability is given.

The remainder of this paper is organized as follows: Section 2 introduces the V2P communication network architecture based on the LSTM and the test environment used in this paper. Section 3 introduces the probabilistic prediction method and the algorithm for judging whether the warning is given, which effectively solves the V2P anticollision problem while considering pedestrian trajectory prediction. In Section 4, the simulation analysis of the algorithm is given, and the real scene tests are carried out by using LoRa equipment to predict pedestrian behavior. Based on the pedestrian's future trajectory, analyze the collision area and collision probability of the pedestrian under different motion trajectories. Finally, the conclusion of this paper is given in Section 5.

2. Autonomous-Oriented V2P Communication Network Architecture

2.1. V2P Communication Network Architecture. This section proposes a three-layer LoRa multiparty collaborative network architecture, including a traffic cloud data center, regional platforms, and terminals, as shown in Figure 1. In addition to data transmission, the network also needs to assist in collaborative computing. The gateway, regional platform, and traffic cloud data center adopt 4G, 5G communication, which evolves to a higher level with the network updates.

The traffic cloud data center realizes the storage and analysis of massive terminals data. The regional platform (including the LoRa network server and edge computing) processes packets received by LoRa gateways, pedestrian terminals, and vehicle terminals in real time. The computational decision unit in edge computing is based on LSTM, which makes the system autonomously and predicts the collision risk more accurately. Because the LSTM enables the V2P system to better solve the problems caused by various pedestrians and the uncertainty of the environment. Most of the functions need to be implemented in the regional platform, checking whether the terminal is online, filtering redundant packets, etc. The terminal is responsible for the collection and transmission of location data. The vehicle terminal includes data collection, data processing, and safety decision-making. The pedestrian terminal and vehicle terminal can interact directly. The data from terminals also can be forwarded through the gateway. This paper does not discuss the vehicle terminal, focusing on the pedestrian terminal.

2.2. Network Server, Gateway, and V2P Pedestrian Terminals. The functions of the network server include communication control, protocol processing, device management, and network maintenance of the LoRa network. The network server helps users register, manage, and monitor LoRa devices, including terminals and gateways. It can also encrypt, decrypt and process application layer payloads. Meanwhile, it can support the application of various encryption or encoding methods to ensure data security and improve transmission efficiency.

The gateway implements the topological link of the LoRa network by receiving data from the terminal and forwarding it to the network server or forwarding the data message from the network server to the terminal.

Pedestrian terminals are used to collect data and send it to the network server through the gateway, or execute commands and tasks from the network server.

Pedestrian terminals and gateways are the foundation of the LoRa network. The gateway can interact with LoRa terminals, collect data such as signal-noise-ratio (SNR), received-signal-strength-indicator (RSSI), and transmit them to the base station for analysis. The terminals can implement different functions according to different application requirements. The gateway uploads all uplink packets to the network server. On the contrary, in the downlink, the LoRa gateway executes the transmission requests from the network server. The gateway usually relays

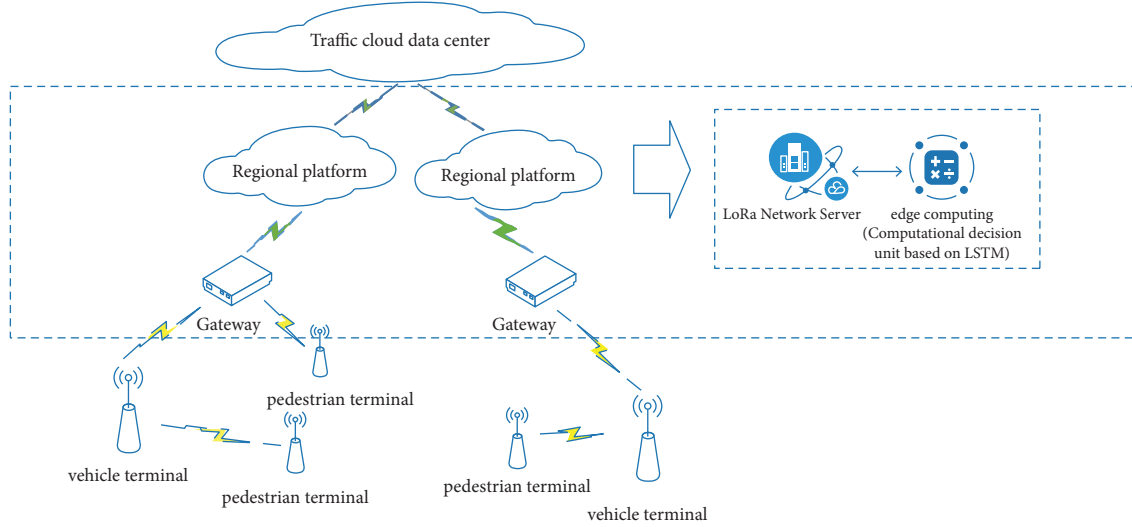


FIGURE 1: LoRa network architecture under the V2P scenario.

the received uplink/downlink packets without processing the payload data. Due to its low-power consumption and long-distance transmission characteristics, the LoRa network provides more reliable terminal location data for the judgment of the V2P communication warning system to improve the accuracy of the system.

2.3. Test Environment. The LoRa system used in the test consists of a gateway and a terminal. The gateway receives and processes messages sent by the terminal. Based on the LoRa network, a test terminal for pedestrians is specially developed. To obtain the position, speed, and direction of the pedestrian and the vehicle, the pedestrian and the vehicle are equipped with GPS to locate them and predict future trajectories based on the pedestrian's past data.

The pedestrian terminal of the test is composed of a LoRa module and GPS with submeter accuracy. The microcontroller unit (MCU) adopts an STM32 chip, the RF module adopts a LoRa RFM98 chip, and the GPS operating frequency is 1 Hz. The hardware frame and physical diagram of the pedestrian terminal are shown in Figure 2. The GPS module and the MCU communicate one way through Universal Synchronous/Asynchronous Receiver/Transmitter (USART). The LoRa module communicates two way with the MCU through the SPI (Serial Peripheral Interface) bus. The hardware frame and physical diagram of the gateway are shown in Figure 3, which consists of four groups of the same module. The gateway can support simultaneous communication with four different frequency bandwidths, in which the LoRa module conducts two-way communication with the MCU through the SPI bus.

The gateway is located on the top of the fifth floor of the building of Xi'an University of Posts and Telecommunications. The pedestrian wears the terminal and walks at a constant speed on the campus. The test path is divided into linear path and nonlinear path.

The paths of the pedestrian wearing the terminal are shown in Figure 4. The actual measurement scene is selected

in Xi'an University of Posts and Telecommunications under the Gaode map. The gateway collects the data and sends it to the network server to map the data on the Gaode map. As shown in Figure 4, the blue is the pedestrian walking trajectory, the left is the linear trajectory, and the right is the nonlinear trajectory.

3. Probabilistic Prediction

3.1. Model of Pedestrian-Vehicle Anticollision. This paper analyzes and models the scene as shown in Figure 5, both the pedestrian (X_p, Y_p) and the vehicle (x_v, y_v) keep moving at a constant speed. The pedestrian is located at the driver's NLOS position and the trajectory is uncertain. The vehicle trajectory tends to be a straight line, and a collision occurs near $p(x, y)$.

Assuming that the pedestrian-vehicle path has a certain angle, the red area $p(x, y)$ in Figure 5 is the area where a collision may occur. The model building will be divided into two steps, minimum safety distance and judgment conditions.

The t_{tot} represents the reaction time for the driver to receive a collision warning and take action.

$$t_{tot} = t_{cesta} + t_{comm d} + t_{react} + t_{resp}, \quad (1)$$

where t_{cesta} is communication connection delay, $t_{comm d}$ is information transmission delay, t_{react} is driver reaction time, and t_{resp} is the time that driver takes action.

3.1.1. Minimum Safety Distance. The minimum safety distance of vehicle anticollision is

$$d = S_1 + S_2 = v_v \cdot t_{tot} + \frac{v_v^2}{2g\mu}, \quad (2)$$

where t_{tot} represents the reaction time for the driver to receive a collision warning and take action. The speed of the vehicle is v_v , s_1 is the distance passed by the driver during the

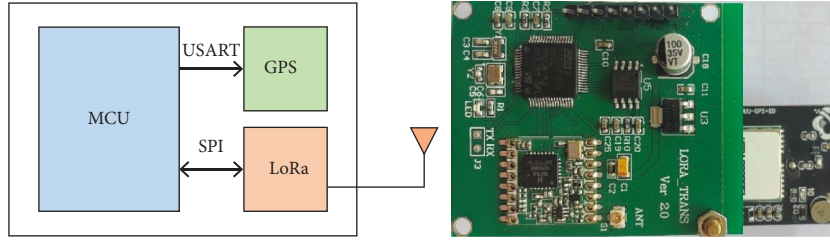


FIGURE 2: Pedestrian terminal (the left is the hardware frame, and the right is the physical diagram).

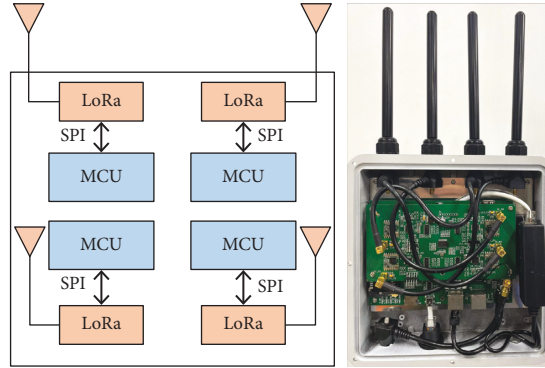


FIGURE 3: Gateway (the left is the hardware frame, and the right is the physical diagram).

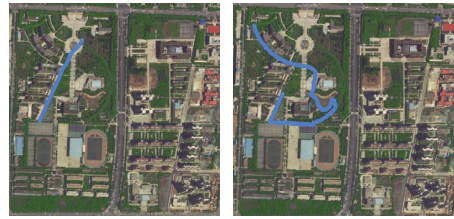


FIGURE 4: Pedestrian path map measured by the pedestrian wearing terminal (at Xi'an university of posts and telecommunications).

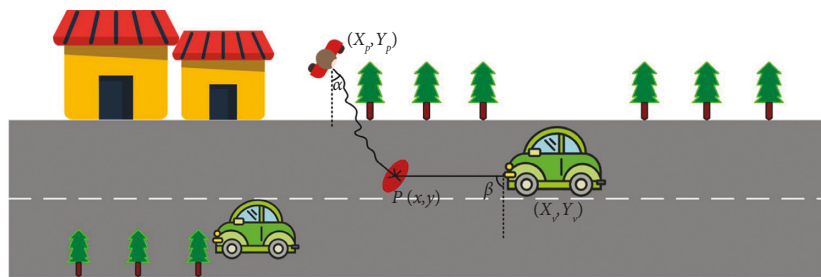


FIGURE 5: Pedestrian-vehicle collision scenario.

period when the driver reacts and takes action, s_2 is the braking distance of the vehicle, $g = 9.8 \text{ m/s}^2$, and μ is the friction coefficient.

3.1.2. *Judgment Conditions.* Obtain two sets of position information (x_1, y_1) , (x_2, y_2) for the pedestrian and (x_3, y_3) , (x_4, y_4) for the vehicle and determine whether there is a collision point $p(x, y)$ through (3).

$$\begin{aligned}
 x &= ((x_3 - x_4) * ((y_1 - y_2) * x_1 - (x_1 - x_2) * y_1) \\
 &\quad - \frac{(x_1 - x_2) * ((y_3 - y_4) * x_3 - (x_3 - x_4) * y_3)}{((y_1 - y_2) * (x_3 - x_4) - (y_3 - y_4) * (x_1 - x_2))}, \\
 y &= ((y_3 - y_4) * ((y_1 - y_2) * x_1 - (x_1 - x_2) * y_1) \\
 &\quad - \frac{(y_1 - y_2) * ((y_3 - y_4) * x_3 - (x_3 - x_4) * y_3)}{((y_1 - y_2) * (x_3 - x_4) - (y_3 - y_4) * (x_1 - x_2))}.
 \end{aligned} \tag{3}$$

The time TTC can be calculated through (4) and (5).

$$TTC = |TTC_V - TTC_p| < \delta, \quad (4)$$

$$\delta = \frac{(W_{car} + d)}{V_v}, \quad (5)$$

where TTC_p is the time that the pedestrian maintains the current speed to the collision point $p(x, y)$, TTC_v is the time that the car maintains the current speed to the collision point $p(x, y)$, W_{car} is the width of the vehicle, and the arrival time difference is δ . δ represents the preset threshold, which determines whether the road condition can be considered dangerous.

Because TTC (the time difference between the pedestrian and the vehicle arriving at the collision point) is not the only factor in determining the potentially dangerous road conditions, the S danger index is also taken into account. This danger index is also considered to decide whether to issue a warning. The danger index S is defined by

$$S(TTC, d) = \begin{cases} \frac{1}{2\pi\sigma^2} \exp\left(-\frac{1}{2} \frac{TTC_v^2}{\sigma^2 d}\right), & \text{collision point } p \text{ exists,} \\ 0, & \text{collision point } p \text{ not exists,} \end{cases} \quad (6)$$

where σ is the accuracy of GPS. According to the typical vehicle speed of 40 km/h, the threshold is divided into two types, 0.01 and 0.1. When the vehicle speed is greater than 40 km/h and S is smaller than 0.01, a warning is given, otherwise, a warning is given when S is smaller than 0.1.

3.2. Trajectory Prediction. Each pedestrian has different movement patterns: speeds, accelerations, and gaits. Therefore, it is necessary to build a model to understand and learn these specific characteristics of pedestrian motion, so as to predict the future trajectories of pedestrians. Neural network is considered to be an effective method to deal with real-time problems, which has been widely used in machine control [34,35] to improve the degree of machine automation [36]. When dealing with the long-term dependence of the input sequence, the traditional RNN network will produce the problem of gradient descent or gradient disappearance. In order to solve this problem, LSTM was proposed by Hochreiter and Schmidhuber [37], and then it was widely used to solve the problem of time series prediction.

LSTM has three gates (update i_t , forget f_t , and output y_t), block input, and memory cells c_t . The output of the block is repeatedly connected back to the input of the block and all gates. The data goes through the horizontal line of the highest point in Figure 6, which is called the cell state. The memory cell uses a function \tanh whose value range is $[-1, 1]$ as the activation function. The forgetting gate controls whether the information in the memory cell of the previous time step is transmitted to the current time step, and the forgetting gate and the memory cell achieve better control of information flow.

In Figure 6, f_t , g_t , i_t , c_t , o_t are

$$\begin{aligned} f_t &= \sigma(\bar{f}_t) = \sigma(W_{xf}x_t + W_{hf}h_{t-1} + b_f), \\ g_t &= \tanh(\bar{g}_t) = \tanh(W_{xg}x_t + W_{hg}h_{t-1} + b_g), \\ i_t &= \sigma(\bar{i}_t) = \sigma(W_{xi}x_t + W_{hi}h_{t-1} + b_i), \\ c_t &= c_{t-1} \odot f_t + g_t \odot i_t, \\ o_t &= \sigma(\bar{o}_t) = \sigma(W_{xo}x_t + W_{ho}h_{t-1} + b_o). \end{aligned} \quad (7)$$

In this paper, the LSTM neural network is used to make cyclic multistep predictions for the future trajectory of the pedestrian. Among them, the activation function is relu , the loss function is MSE, the optimizer is Adam, the metric is accuracy, and the epoch is 100. GPS location information (latitude and longitude) of the pedestrian is used as the input of the LSTM. The cross-validation method is used for machine learning to improve the accuracy of machine learning and avoid overfitting and underfitting. The output is the location information, mean, and covariance of the pedestrian's future trajectory.

3.3. Collision Probability. The mean and covariance of the pedestrian's future trajectory can be obtained by LSTM for trajectory prediction, which can indicate the predicted area that the car needs to avoid, called the collision area R . For the i th pedestrian's movement, it is assumed that the probability of its future location at a certain position depends on the collision area R_i at time t , and R_i is based on the mean $\mu_i(t) = [\mu_x, \mu_y]^T$ and covariance $\sum_i(t) = \mathbb{R}^{2 \times 2}$ at time t . For convenience, the variable t will be ignored in the following description of this chapter, so that we can assume that the future position of the i^{th} pedestrian moving at time t can be expressed as $P_{i,f} \sim N(\mu_i, \sum_i)$.

Remark 1. Since the covariance matrix \sum_i is a real symmetric, positive semi-definite matrix, and the eigenvalues are real numbers, there is an orthogonal matrix Q_i composed of the eigenvectors \sum_i . The eigenvalues of the covariance matrix \sum_i can be decomposed into

$$\sum_i = Q_i \Lambda_i Q_i^T, \quad (8)$$

where $\Lambda_i = \text{diag}(\lambda_j)$, $j = 1, 2$, λ_j sort in descending order, $\lambda_1 \geq \lambda_2$, j represents a dimension in the environment.

In this section, two key results (on the construction of the ellipse and the calculation of scaling factors) need to be explained, which are crucial parts of the model prediction.

Lemma 1. *An ellipse can be constructed from a transformation of the unit circle by first stretching it along each axis with the ratio $\sqrt{\lambda_i}$, then rotating the ellipse through Q_i , and finally translating the center m_i of the distribution to the origin according to the following inverse Mahalanobis transformation:*

$$R_i = Q_i \Lambda_i^{1/2} Q_i^T u + \mu_i, \quad (9)$$

where $u \sim N(0, I_2)$ is the unit circle of a two-dimensional normal distribution. In this paper, I_2 denotes the identity matrix with the size of 2×2 .

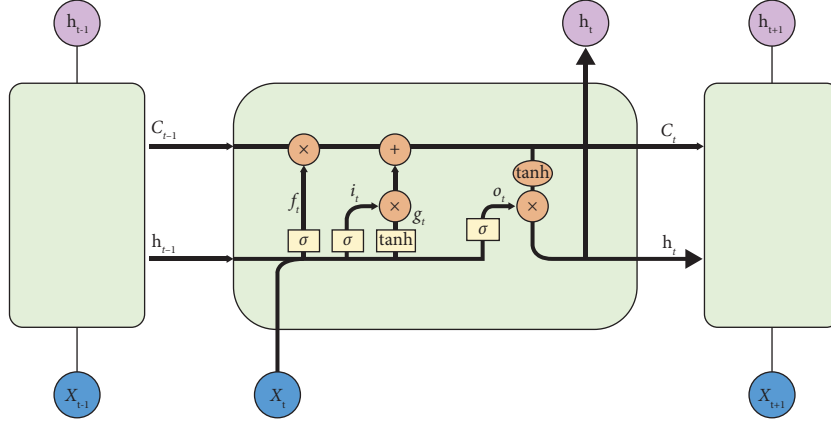


FIGURE 6: Repeating modules in LSTM (i_t is update gate, f_t is forget gate, and y_t is output gate).

Proof. Mapping a unit circle by the square root of the covariance matrix, $\sum_i^{1/2}$ determines an ellipse whose principle semiaxes depend on the eigenvalues of this matrix, and whose direction is related to the corresponding eigenvectors. To represent this ellipse graphically, the Mahalanobis transform eliminates the correlation between variables and normalizes each variable by its variance. Therefore, an ellipse can be constructed from the transformation of the unit circle, according to the inverse Mahalanobis transformation (9).

Next here, the scaling factor is calculated and the confidence probability that the collision area is an ellipse is derived. \square

Lemma 2. *The scaling factor r can be calculated approximately by*

$$F(r) = P(r) - \Phi,$$

$$\tilde{F}(r) = \tilde{P}(r) = \sqrt{\frac{2}{\pi}} \exp\left(-\frac{r^2}{2}\right) + \frac{\exp(-r^2/2)}{\sqrt{2}\Gamma(3/2)}(r^2 - 1). \quad (10)$$

Proof. Based on Lemma 2, the square of the Mahalanobis distance (scaling factor r) of the possible positions $P_{i,f}$ to its mean μ_i can be calculated by

$$r^2 = (P_{i,f} - m_i)^T \sum_i^{-1} (P_{i,f} - m_i). \quad (11)$$

Bring into the above equation through (8) and (9), the magnified ellipse with scaling factor r can be obtained, relying on the chi-square χ^2 distribution with the degree of freedom $\sigma = 2$, as shown in

$$\Pr(r^2 \leq \chi_{\sigma=2,p}^2) = \Phi, \quad (12)$$

which can be expressed as

$$\Pr\left(\left(a_{i,f} - \mu_i\right)^T \sum_i^{-1} \left(a_{i,f} - \mu_i\right) \leq r^2\right) = \Pr(u^T u \leq r^2). \quad (13)$$

The confidence probability for an arbitrary ellipse with any factor r can be calculated, as shown in

$$\begin{aligned} P(r) &= \Pr(u^T u \leq r^2) \\ &= \iint 2\pi^{-(3/2)} \exp\left(-\frac{u_1^2 + u_2^2}{2}\right) du_1 du_2, \quad (14) \\ &= \operatorname{erf}\left(\frac{r}{\sqrt{2}}\right) - \left(\frac{r}{\sqrt{2}}\right) \frac{\exp(-r^2/2)}{\Gamma(3/2)}, \end{aligned}$$

where

$$\operatorname{erf}(x) = \frac{2}{\sqrt{\pi}} \int_0^x \exp(-t^2) dt, \quad (15)$$

is the standard error function and Γ is the gamma function. The scaling factor $r = 2.7955, 3.3682$ when the corresponding confidence probabilities $P(r) = 95\%, 99\%$, respectively. \square

3.4. Algorithm Description. The system obtains the location information of pedestrians and vehicles in real time, uses LSTM to predict the future trajectory of the pedestrian, and obtains the probability density function of the pedestrian trajectory, which obeys a multidimensional normal distribution function. It preliminarily infers the collision area between the pedestrian and the vehicle, and finally uses the confidence probability to determine whether to give a warning to the pedestrian and the vehicle.

In practice, in order to better describe the real data D_{real} , adding a normal distribution function to ideal data D to approximate real data D_{real}

$$D_{\text{real}} = D + N(\mu, \sigma). \quad (16)$$

The system algorithm description is as follows (Algorithm 1):

4. Result Analysis

4.1. Influencing Factors of System Collision Risk Warning Time. The influence of GPS positioning error, vehicle speed, and other uncertain factors on the anticollision

Input: Two sets of GPS data for pedestrian and vehicle

Output: A risk of collision occurs or not

- (1) Acquire 2 sets of GPS data continuously (pedestrian and vehicle) $(X_{p1}, Y_{p1}), (X_{p2}, Y_{p2}), (X_{v1}, Y_{v1}), (X_{v2}, Y_{v2})$
 if there is a collision point $p(p_x, p_y)$
 if $TTC = |TTC_v - TTC_p| < \delta$ and $\delta = (W_{car} + d)/V_v$
 if the confidence probability corresponding to the collision area generated by the predicted future trajectory $P(r) > 95\%$
 Output: A risk of collision will occur.
- (2) Calculate the direction angle of pedestrian and vehicle α, β
 if $0 < |\alpha| < 90^\circ$ or $0 < |\beta| < 90^\circ$
 $\max\{X_{p2}, X_{p2}, X_{v1}, X_{v2}\} > P_x$, stop getting data
 else
 $\min\{X_{p2}, X_{p2}, X_{v1}, X_{v2}\} < P_x$, stop getting data

ALGORITHM 1: Collision warning.

system model is studied through the simulation. The simulation scene is shown in Figure 5. The pedestrian and the vehicle start at the same time and keep running at a uniform speed. It is assumed that the collision occurs 200 seconds after the pedestrian and vehicle movement. In order to be closer to the actual situation, the error is added to the position data during simulation. This paper assumes that the error obeys the normal distribution. The pedestrian speed is 1 m/s, and the driving speed is variable. The reaction time t_{tot} for the driver receiving the collision warning and taking action is 0.83 s [38], the friction coefficient μ is 0.8, and the vehicle length is 5 m.

According to the idea of control variables, by setting different GPS positioning errors and driving speeds, the change of the warning time of pedestrian-vehicle collision risk is analyzed as follows.

4.1.1. The Relationship between Driving Speed and Collision Risk Assessment Time. Control the GPS positioning error $\sigma = 1$, i.e., the error is 1 m, and the driving speed is changed. The changing relationship of collision risk assessment time is compared when the driving speed is 30 km/h, 40 km/h, and 60 km/h. The difference of collision risk assessment time under the different vehicle speeds is shown in Figure 7. The horizontal axis is the time in seconds. The vertical axis is the time difference between the vehicle and the pedestrian arriving at the collision point, and the unit is second. The coordinates marked in Figure 7 are the warning time and TTC . The higher the speed, the earlier the collision warning. In Figure 7(a), when the driving speed is 30 km/h, the time difference between the pedestrian and the vehicle arriving at the collision point is 1.96 s, and the system sends out a danger warning in 198 s, i.e., 2 seconds in advance. In Figure 7(c), when the driving speed is 60 km/h, the time difference between the pedestrian and the vehicle arriving at the collision point is 2.19 s, and the system issues a danger warning in 195 s. When the positioning error is 1 meter, a warning is given at typical speeds within 2 to 5 seconds before the collision point arrives, and the results show that the algorithm is feasible.

4.1.2. The Effect of GPS Positioning Error on the Collision Risk Assessment Time. Change the GPS positioning accuracy when the vehicle speed is constant and compare the changing relationship of the collision risk early warning evaluation time when the positioning accuracy is 1 m and 10 m. Under different GPS positioning errors, the collision risk assessment time is different as shown in Figure 7. The positioning errors in Figures 7(a)–7(c) are 1 m, and the positioning errors in Figures 7(d)–7(f) are 10 m. The greater the GPS positioning error, the earlier the collision warning. In Figures 7(a), 7(d), when the vehicle speed is 30 km/h, the time difference between the pedestrian and the vehicle reaching the collision point is 1.96 s when the positioning accuracy is 1 m and 10 m, and the system issues a danger warning in 190 s. When the vehicle speed is 60 km/h, the time difference between the pedestrian and the vehicle reaching the collision point is 2.19 s, and the system sends a hazard warning in the 180 s. The results show that the positioning error does not affect the time difference of arrival, but only affects the warning time. Because the danger index should be considered in the warning, and the danger index is related to the positioning error.

4.2. Collision Area and Corresponding Confidence Probability. Based on the anticollision model, when v_v is 30 km/h, 40 km/h, or 60 km/h, the warning time is obtained when the GPS positioning error $\sigma = 1$ is used. 500×4 and 1250×2 sample data are used for straight line and nonstraight line, respectively. The sample data are predicted by LSTM. After the model training is completed, the prediction takes only 1~2 seconds, which can meet the application requirements. This is because only one set of data is predicted per round, so the prediction time is faster. The units in Tables 2 and 3 are meters. In this paper, 10.2.1 represents the use of ten data to predict the pedestrian position after two seconds, i.e., the first number 10 is the number of data used by the LSTM, the second number 2 is the position data predicted by the LSTM after 2 seconds, and the third number 1 represents the 1 position data predicted by the LSTM. If the pedestrian keeps moving in a straight line, using 6 seconds or 10 seconds to predict the position offset after multiple steps is 0 meters, but for nonlinear situations, it is better to use ten seconds to predict the position

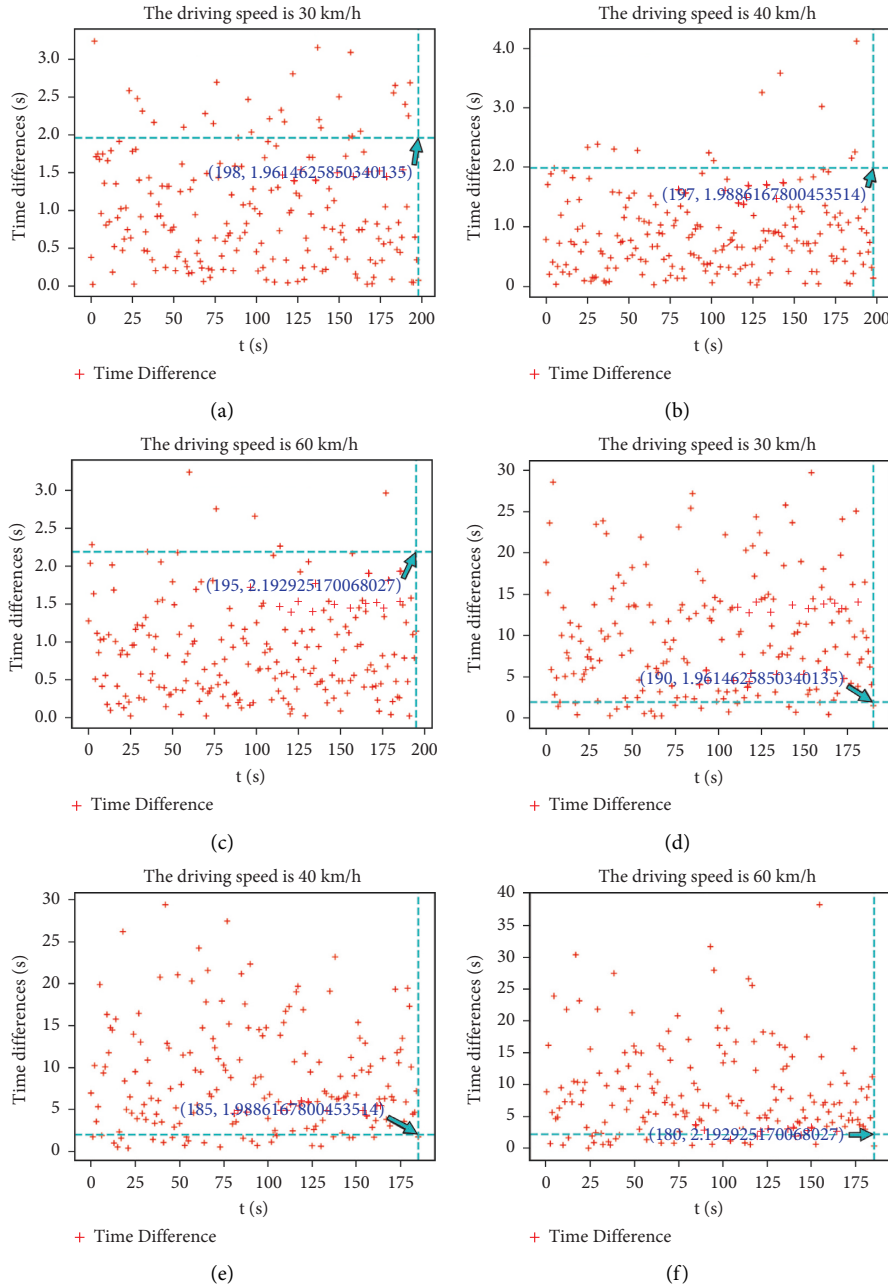


FIGURE 7: The influence of system positioning accuracy on the pedestrian collision risk detection (a, b, c positioning error is 1 m, d, e, f positioning error is 10 m).

TABLE 2: Pedestrian future trajectory prediction error.

	Linear (m)	Nonlinear (m)
6.5.1	0.0	11.3
6.2.1	0.0	7.6
10.5.1	0.0	1.5
10.2.1	0.0	0.6

TABLE 3: Collision area and corresponding confidence probability.

	Linear (m) (%)	Nonlinear (m) (%)
6.5.1	98.61	99.39
6.2.1	99.57	99.39
10.5.1	99.12	99.2
10.2.1	99.57	99.73

after multiple steps. This is because when the pedestrian trajectories are nonlinear, machine learning needs to learn more features, so more data are required. At the same time, the accuracy of the algorithm is also verified.

Here, a nonlinear prediction trajectory in 6.5.1 is used as an example to describe the prediction performance. The collision area of the uncertainty position prediction method is described in Figure 8. If the vehicle continues in its current

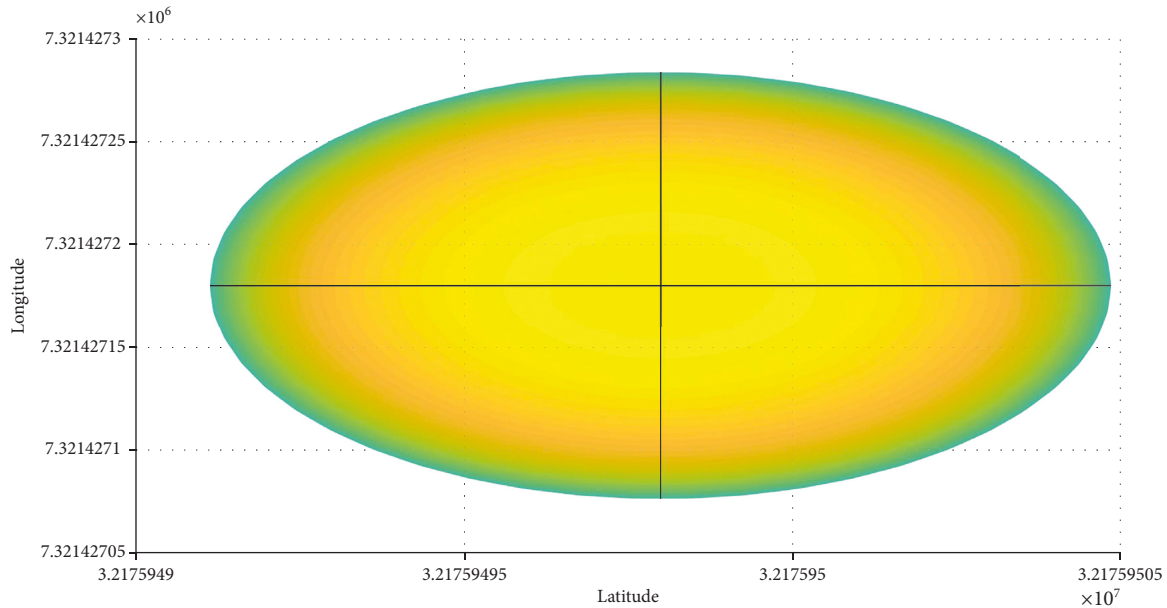


FIGURE 8: The collision area corresponding to a predicted trajectory (the horizontal and vertical coordinates are the latitude and longitude after mapping the Miller coordinate system to the plane coordinate system).

state, it will collide with the pedestrian in the collision zone with a probability of 99.39%. Among them, the center point of the ellipse is the mean value, and the colored area is the collision area. The closer to the center point, the smaller the covariance and the higher the probability of collision.

5. Conclusions

This work focuses on the problems caused by the uncertainty of pedestrian trajectory in the V2P scene, such as the determination of the collision area and the calculation of the collision probability. To do so, this paper proposed a new communication network architecture and V2P collision warning system. The system considers the GPS positioning accuracy, typical vehicle speed, the uncertainty of pedestrian behavior, and introduces a danger index to measure the degree of risk. The pedestrian behavior is predicted by using LSTM to set the collision area and gives the corresponding confidence probability. The simulation shows the influence of positioning accuracy and the vehicle speed on the warning time, which is left to the driver as the reaction time to take measures. The test gives the collision area and the corresponding confidence probability. Compared with the existing literature, the proposed method is to systematically realize the early warning system. The designed V2P early warning system is feasible for effectively improving road traffic safety and has certain reference value and practical significance for pedestrian safety protection research. The results have strong generality and reliability and can be applied to more common pedestrian and vehicle scenarios.

The proposed research method is applicable to the communication problem between a vehicle and a pedestrian. For future work, we are working on the problem of communication between multiple vehicles and multiple

pedestrians. It is proposed to use filters to obtain the vehicle and the pedestrian with collision risk.

Data Availability

The data used to support the findings of this study are available from the corresponding author upon reasonable request.

Conflicts of Interest

The authors declare no conflicts of interest.

Acknowledgments

This work was supported by the Key Industry Innovation Chain Project of Shaanxi Province (nos. 2021ZDLGY07-10 and 2021ZDLNY03-08), the Science and Technology Plan Project of Shaanxi Province (no. 2022GY-045), Natural Science Foundation of Shaanxi Province (no. 2020JM-537), the Key Research and Development Plan of Shaanxi Province (no. 2018ZDXM-GY-041), Scientific Research Program Funded by Shaanxi Provincial Education Department (Program no. 21JC030), the Science and Technology Plan Project of Xi'an (no. 2019GXYP17.3), and Graduate Innovation Fund of Xi'an University of Posts and Telecommunications (CXJLZ202018).

References

- [1] Y. Ma, X. Zhu, S. Zhang, R. Yang, W. Wang, and D. Manocha, "TrafficPredict: trajectory prediction for heterogeneous traffic-agents," in *Proceedings of the AAAI Conference on Artificial Intelligence*, Hawaii, U.S.A., February 2019.
- [2] C. Chen, Y. R. Zhang, Z. Wang, S. Wan, and Q. Pei, "Distributed computation offloading method based on deep

- reinforcement learning in ICV,” *Applied Soft Computing*, vol. 103, Article ID 107108, 2021.
- [3] P. A. Hancock, I. Nourbakhsh, and J. Stewart, “On the future of transportation in an era of automated and autonomous vehicles,” *Proceedings of the National Academy of Sciences*, vol. 116, no. 16, pp. 7684–7691, 2019.
 - [4] A. Rasouli and J. K. Tsotsos, “Autonomous vehicles that interact with pedestrians: a survey of theory and practice,” *Proceedings of IEEE Transactions on Intelligent Transportation Systems*, vol. 21, no. 3, pp. 26–29, 2019.
 - [5] A. Hussein, F. García, J. M. Armingol, and O. M. Cristina, “P2V and V2P communication for Pedestrian warning on the basis of Autonomous Vehicles,” in *Proceedings of the IEEE 19th International Conference on Intelligent Transportation Systems (ITSC)*, pp. 1–4, LeblonRio de Janeiro, Brazil, November 2016.
 - [6] W. Cunningham, “Honda tech warns drivers of pedestrian presence,” 2017, <https://www.cnet.com/%20roadshow/news/honda-tech-warns-drivers-of-pedestrian-presence/>.
 - [7] Who, “Global Status Report on Road Safety 2018: Summary,” Technical. Report, World Health Organization (WHO), Geneva, 2018.
 - [8] R. Q. Malik, K. N. Ramli, Z. H. Kareem, M. I. Habelalmatee, A. H. Abbas, and A. Alamoody, “An overview on V2P communication system: architecture and application,” in *Proceedings of the International Conference on Engineering Technology and its Applications (IICETA)*, pp. 6-7, Najaf, Iraq, September 2020.
 - [9] D. Steinhäuser, P. Held, B. Thoresz, and T. Brandmeier, “Towards safe autonomous driving: challenges of pedestrian detection in rain with automotive radar,” in *Proceedings of the 17th European Radar Conference (EuRAD)*, Utrecht, Netherlands, January 2021.
 - [10] B. Lv, R. Sun, H. Xu, and R. Yue, “Automatic vehicle-pedestrian conflict identification with trajectories of road users extracted from roadside lidar sensors using a rule-based method,” *IEEE Access*, vol. 7, pp. 161594–161606, 2019.
 - [11] C. Y. Li, G. Salinas, P. H. Huang, G. H. Tu, G. H. Hsu, and T. Y. Hsieh, “V2PSense: enabling cellular-based V2P collision warning service through mobile sensing,” in *Proceedings of the IEEE International Conference on Communications (ICC)*, pp. 20–24, Kansas City, MO, U.S.A, May 2018.
 - [12] D. Olmeda, C. Premevida, U. Nunes, J. M. Armingol, and A. D. L. Escalera, “Pedestrian detection in far infrared images,” *Integrated Computer-Aided Engineering*, vol. 20, no. 4, pp. 347–360, 2013.
 - [13] A. Prioletti, A. Mogelmoose, P. Grisleri, M. M. Trivedi, A. Broggi, and T. B. Moeslund, “Part-based pedestrian detection and feature-based tracking for driver assistance: real-time, robust algorithms, and evaluation,” *IEEE Transactions on Intelligent Transportation Systems*, vol. 14, no. 3, pp. 1346–1359, 2013.
 - [14] F. García, J. García, A. Ponz, J. M. Armingol, and A. D. L. Escalera, “Context aided pedestrian detection for danger estimation based on laser scanner and computer vision,” *Expert Systems with Applications*, vol. 41, no. 15, pp. 6646–6661, 2014.
 - [15] S. H. Sun, J. L. Hu, Y. Peng, X. M. Pan, L. Zhao, and J. Y. Fang, “Support for vehicle-to-everything services based on LTE,” *IEEE Wireless Communications*, vol. 23, no. 3, pp. 4–8, 2016.
 - [16] L. Kong, L. Ye, F. Wu, M. Tao, G. Chen, and A. V. Vasilakos, “Autonomous relay for millimeter-wave wireless communications,” *IEEE Journal on Selected Areas in Communications*, vol. 35, no. 9, pp. 2127–2136, 2017.
 - [17] T. S. Rappaport, Y. Xing, G. R. MacCartney, A. F. Molisch, E. Mellios, and J. Zhang, “Overview of millimeter wave communications for fifth-generation (5G) wireless networks—with a focus on propagation models,” *IEEE Transactions on Antennas and Propagation*, vol. 65, no. 12, pp. 6213–6230, 2017.
 - [18] P. Merdrignac, O. Shagdar, and F. Nashashibi, “Fusion of perception and V2P communication systems for the safety of vulnerable road users,” *IEEE Transactions on Intelligent Transportation Systems*, vol. 18, no. 7, pp. 1740–1751, 2017.
 - [19] U. Raza, P. Kulkarni, and M. Sooriyabandara, “Low power wide area networks: an overview,” *IEEE Communications Surveys & Tutorials*, vol. 19, no. 2, pp. 855–873, 2017.
 - [20] J. Petajajarvi, K. Mikhaylov, M. Hamalainen, and J. Iinatti, “Evaluation of LoRa LPWAN technology for remote health and wellbeing monitoring,” in *Proceedings of the 10th International Symposium on Medical Information and Communication Technology (ISMICT)*, Worcester, MA, U.S.A, March 2016.
 - [21] S. S. Magdum, A. Franklin, B. R. Tamma, and D. S. Pawar, “SafeNav: a cooperative V2X system using cellular and 802.11p based radios opportunistically for safe navigation,” in *Proceedings of the 2020 IEEE 23rd International Conference on Intelligent Transportation Systems (ITSC)*, Rhodes, Greece, September 2020.
 - [22] Y. Ren, Z. Zhao, Q. Yang, and K. S. Hong, “Adaptive neural-network boundary control for a flexible manipulator with input constraints and model uncertainties,” *IEEE Transactions on Cybernetics*, vol. 51, no. 10, pp. 4796–4807, 2021.
 - [23] Z. J. Liu, J. Shi, X. N. Zhao, and H. X. Li, “Adaptive fuzzy event-triggered control of aerial refueling hose system with actuator failures,” *IEEE Transactions on Fuzzy Systems*, 2021.
 - [24] Z. Liu, L. Pu, Z. Meng, X. Yang, K. Zhu, and L. Zhang, “POFS: a novel pedestrian-oriented forewarning system for vulnerable pedestrian safety,” in *Proceedings of the 2015 International Conference on Connected Vehicles and Expo (ICCVE)*, pp. 19–23, Shenzhen, China, October 2015.
 - [25] P. Ho and J. Chen, “WiSafe: wi-fi pedestrian collision avoidance system,” *IEEE Transactions on Vehicular Technology*, vol. 66, no. 6, pp. 4564–4578, 2017.
 - [26] G. Xiog, T. Yang, M. Li, Y. Zhang, W. Song, and J. Gong, “A novel V2X-based pedestrian collision avoidance system and the effects analysis of communication delay and packet loss on its application,” in *Proceedings of the 2018 IEEE International Conference on Vehicular Electronics and Safety (ICVES)*, vol. 12, Madrid, Spain, September 2018.
 - [27] R. Bastani Zadeh, M. Ghatee, and H. R. Eftekhari, “Three-phases smartphone-based warning system to protect vulnerable road users under fuzzy conditions,” *IEEE Transactions on Intelligent Transportation Systems*, vol. 19, no. 7, pp. 2086–2098, 2018.
 - [28] B. I. Sighencea, R. I. Stanciu, and C. D. Căleanu, “A review of deep learning-based methods for pedestrian trajectory prediction,” *Sensors*, vol. 21, no. 22, p. 7543, 2021.
 - [29] Y. M. Jiang, Y. N. Wang, and Z. Miao, J. Na, Z. Zhao, and C. Yang, “Composite-learning-based adaptive neural control for dual-arm robots with relative motion,” *IEEE Transactions on Neural Networks and Learning Systems*, vol. 33, no. 3, pp. 1010–1021, 2022.
 - [30] G. Q. Zhang, J. Li, X. Jin, and C. Liu, “Robust adaptive neural control for wing-sail-assisted vehicle via the multiport event-triggered approach,” *IEEE Transactions on Cybernetics*, pp. 1–13, 2021.

- [31] C. Chen, J. G. Jiang, and Y. Zhou, N. Lv, X. Liang, and S. Wan, "An edge intelligence empowered flooding process prediction using Internet of things in smart city," *Journal of Parallel and Distributed Computing*, vol. 165, pp. 66–78, 2022.
- [32] M. Kamel, J. Alonso-Mora, R. Siegwart, and J. Nieto, "Robust collision avoidance for multiple micro aerial vehicles using nonlinear model predictive control," in *Proceedings of the 2017 IEEE/RSJ International Conference on Intelligent Robots and Systems (IROS)*, pp. 24–28, Vancouver, Canada, September 2017.
- [33] R. Pepy and A. Lambert, "Safe path planning in an uncertain-configuration space using RRT," in *Proceedings of the 2006 IEEE/RSJ International Conference on Intelligent Robots and Systems*, vol. 9, Beijing, China, October 2006.
- [34] G. Q. Zhang, S. Liu, J. Q. Li, and X. Zhang, "LVS guidance principle and adaptive neural fault-tolerant formation control for underactuated vehicles with the event-triggered input," *Ocean Engineering*, vol. 229, Article ID 108927, 2021.
- [35] Z. J. Zhao, Y. Ren, C. Mu, T. Zou, and K. S. Hong, "Adaptive neural-network-based fault-tolerant control for a flexible string with composite disturbance observer and input constraints," *IEEE Transactions on Cybernetics*, 2021.
- [36] C. X. Liu, G. L. Wen, Z. Zhao, and R. Sedaghati, "Neural-network-based sliding-mode control of an uncertain robot using dynamic model approximated switching gain," *IEEE Transactions on Cybernetics*, vol. 51, no. 5, pp. 2339–2346, 2021.
- [37] S. Hochreiter and J. Schmidhuber, "Long short-term memory," *Neural Computation*, vol. 9, no. 8, pp. 1735–1780, 1997.
- [38] K. David and A. Flach, "CAR-2-X and pedestrian safety," *IEEE Vehicular Technology Magazine*, vol. 5, no. 1, pp. 70–76, 2010.